

Numerical Simulation of Contra Rotating Propellers

Feng Feng, Chong Geng, Ting Guo, Qing-yuan Huang and Jian Hu*

College of Shipbuilding Engineering, Harbin Engineering University, Harbin, 150001, China

*Corresponding Author

Keywords: Contra-rotating Propeller ,Hydrodynamic Performance, CFD, Induced Velocity

Abstract: In this paper, numerical simulation based on Reynolds-averaged Navier-Stokes (RANS) equation and $k-\omega$ SST turbulence model is performed to investigate the hydrodynamic performance of Contra rotating propeller (CRP). The whole computation domain is divided into three sub-domains, which include the two rotating domains containing the fore and aft propellers, and the left outer domain. MRF (Multiple reference frame) coordinate system technique is used to simulate the rotation of the propeller. Fully structured gridding strategy is used to ensure the accuracy of the calculation and reduce computation time. The numerical simulation is verified by the experimental data of CRP6 and CRP7. Then, further analysis of the fluctuation of the thrust and torque is performed, as well as the hydrodynamic interference between the two forward and aft propellers.

Introduction

Fuel cost of propulsion occupies the largest portion of ship operation cost. Thus, it is important to improve energy-saving devices. Among the various devices, the contra-rotating propellers behave high efficiency compared with a single propeller. In the contra-rotating propellers system, the aft propeller could recover a part of the energy loss of fore propeller, which could significantly improve the propulsion efficiency. Thus a numerical simulation is used to discuss the hydrodynamic interaction of contra rotating propellers.

Related the present problem, Yang et al. [1] used a wake model for single propeller with modification to determine the trailing vortex geometry of contra-rotating propellers. The trailing vortex pitches are determined by aligning the trailing vortices to the circumferentially averaged flow far behind the propellers. Using the linearized lifting surface theory, Tsakonas et al. [2] developed a method to predict the steady and unsteady performances of contra-rotating propellers.

Keh-Sik Min et al. [3] had performed studies on the CRP system, and some of the results from the studies were presented and discussed. Stuermer [4] made a detailed analysis of the complex aerodynamic interactions between the two rotors as well as an in-depth analysis of the blade and rotor forces. In order to assess the static and dynamic response of an aft propeller of Contra rotating propeller (CRP) for entire range of its operation, Suryanarayana et al. [5] made an analysis using finite element method validated it by analytical approach.

The above mentioned works on the present problem are mainly based on potential flow assumption and the governing equations are solved by boundary element method. It is well known that this method can not account for the fluid viscosity and flow separation. Thus, in this paper, the commercially available software Star CCM+ is applied in the present simulation. The numerical results are verified by experimental data. On this basis, extensive simulation is performed the hydrodynamic performance of contra rotating propellers.

Methodology

Governing Equations

The Euler form of mass conservation equation can be expressed as following

$$\frac{\partial \rho}{\partial t} + \frac{\partial(\rho u)}{\partial x} + \frac{\partial(\rho v)}{\partial y} + \frac{\partial(\rho \omega)}{\partial z} = 0 \quad (1)$$

in which, ρ is the density of fluid; t is time, u, v and ω is the velocity component in x, y and z directions.

Generally speaking, momentum conservation equation is also called N-S equation, its expression can be written as Eq. 2

$$\begin{aligned} \frac{\partial(\rho u)}{\partial t} + \text{div}(\rho \mathbf{u} u) &= -\frac{\partial \rho}{\partial x} + \frac{\partial \tau_{xx}}{\partial x} + \frac{\partial \tau_{yx}}{\partial y} + \frac{\partial \tau_{zx}}{\partial z} + F_x \\ \frac{\partial(\rho v)}{\partial t} + \text{div}(\rho \mathbf{u} v) &= -\frac{\partial \rho}{\partial y} + \frac{\partial \tau_{xy}}{\partial x} + \frac{\partial \tau_{yy}}{\partial y} + \frac{\partial \tau_{zy}}{\partial z} + F_y \\ \frac{\partial(\rho \omega)}{\partial t} + \text{div}(\rho \mathbf{u} \omega) &= -\frac{\partial \rho}{\partial z} + \frac{\partial \tau_{xz}}{\partial x} + \frac{\partial \tau_{yz}}{\partial y} + \frac{\partial \tau_{zz}}{\partial z} + F_z \end{aligned} \quad (2)$$

In which, τ_{xx}, τ_{xy} and τ_{xz} is tangential stress in different direction due to the viscosity of fluids, F_x, F_y and F_z is the mass forces.

Numerical Model

Well known $k-\omega$ SST model is applied in the present simulation. The model results from the modification of wilcox $k-\omega$ model. The model has been accurate and computational efficient, especially in the simulation of near wall fluid motion. The $k-\omega$ SST model can be written as

$$\frac{Dt}{D}(\rho \omega) = \alpha \left(\frac{\omega}{k}\right) P_k - \beta_w \rho \omega^2 + \frac{\partial}{\partial x_i} ((\mu + \sigma_\omega \mu_t) \frac{\partial \omega}{\partial x_i}) \quad (3)$$

in which, β_w, σ_ω and α is empirical parameter, ρ is density, μ_t is eddy viscosity, k is turbulence energy, P_k is turbulence kinetic energy k generated, ω is specific turbulent dissipation rate, t is time.

Meshing Strategy

Based on the aforementioned numerical method, numerical simulation of CRP6 is performed. The geometric particulars of CRP6 is listed in Tab. 1

Table 1. Geometrical Particulars of CRP6

	Forward Prop.	Aft Prop.
Diameter (mm)	305.2	299.1
Number of Blades	4	4
Expanded Area Ratio	0.303	0.324
Boss Ratio	0.2	0.2041
Pitch at 0.7R (mm)	394	396.8
Rotating Direction	Right-handed	Left-handed

The dimension of the computational domain is shown in Fig. 1. The velocity inlet and pressure outlet boundaries conditions are imposed on the longitudinal ends the computational domain. The total domain is divided into three sub-domains, including two rotating sub-domains containing the fore and aft propeller and the left stationary sub-domain. The orthogonal meshing is shown in Fig. 3. In the vicinity of the propellers, the flow is strongly disturbed and intenser gridding is imposed. In this paper, trimmed mesh is used for the body surface, for which prismatic mesh is used for resolving the boundary layer. The first cell height off both propellers' surface is approximately $0.00001D$, which is 30 to 50 in terms of y^+ , and the number of prism layer is 3 with stretching ratio for 1.5.

The Reynolds-average Navier-Stokes(RANS) equations for mass and momentum transfer are solved on the whole computational domain around the contra-propeller. The two-equation K- ω SST turbulence model is selected to describe the turbulence A segregated solution with SIMPLE-type algorithm for velocity-pressure coupling model is applied for transport equations. All the under-relaxation factors are assumed to take default values, specifically, the value for velocity is 0.8, for pressure 0.2, for turbulent viscosity 1.0.

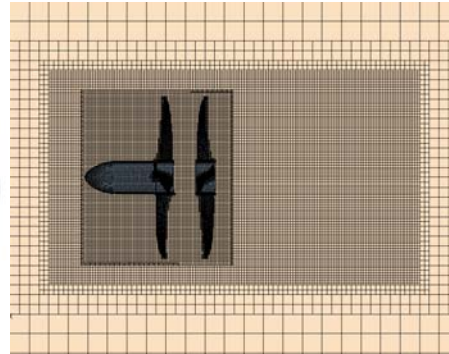
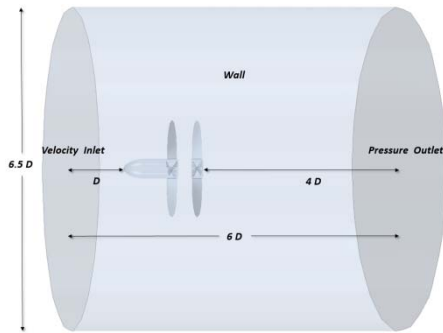


Figure 1. Dimension of the computational domain

Figure 2. Transverse view of meshing

Convergence Study

For clarity and convenience in the following discussion, the advance velocity coefficient, thrust coefficient, torque coefficient are defined as following.

$$K_T = \frac{T}{\rho n^2 D^4} \quad K_Q = \frac{Q}{\rho n^2 D^5} \quad J = \frac{V}{nD} \quad \eta = \frac{JK_T}{2\pi K_Q} \quad C_p = \frac{P}{\frac{1}{2} \rho (V_A^2 + 2\pi n r^2)} \quad (8)$$

Where ρ water density, N propeller revolutions per seconds, D propeller diameter, V inflow velocity, K_T and K_Q are non-dimensional thrust and torque respectively, J is advance coefficient and η is operating efficiency.

Numerical independency of numerical results is critical in the simulation and verified in Tab. 2 and Tab. 3 for CRP6 as $J=0.7$. In Tab. 2, three time steps are used in the verification, which are 0.001s, 0.0005s and 0.0002s, corresponding to 4.32, 2.16 and 0.864 rotational degrees respectively. Form Tab. 1, it can be seen the relative error of 0.0005s and 0.0002s with respect to 0.001s are very small and negligible. Similar conclusion can be obtained for the grid number through the comparison in Tab. 3. In the following simulation, the time step is 0.0002s and the grid number is 5.18 million.

Table 2. Comparison of the theoretical values at three time steps

Time step(s)		Forward		Aft	
		Ktf	10Kqf	Kta	10Kqa
0.001	Cal.	0.08223	0.08874	0.14612	0.16846
0.0005	Cal.	0.08233	0.08910	0.14624	0.16870
	Error(%)	0.116%	0.406%	0.087%	0.143%
0.0002	Cal.	0.08246	0.08932	0.14641	0.16885
	Error(%)	0.274%	0.653%	0.200%	0.231%

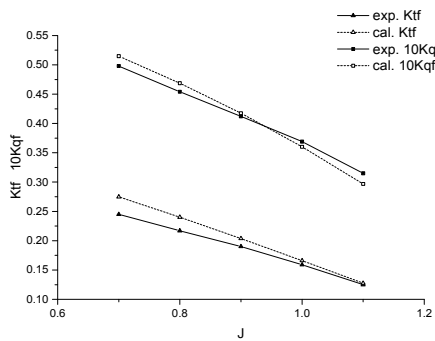
Results and Discussion

The comparison of the open-water performances obtained from the simulations with experimental data for $J=0.7, 0.8, 0.9, 1.0$ and 1.1 is shown in Figure . It is obvious that the calculated value is slightly higher than the experimental value for the thrust coefficient of fore

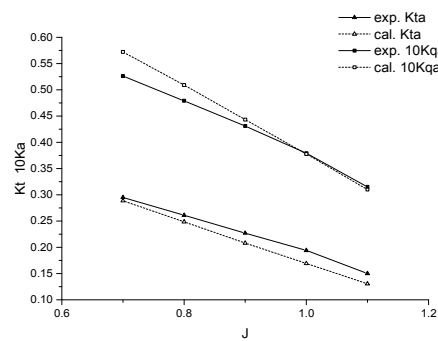
propeller. The average error is 7.302% and the maximum error reach 12.214% for $J=0.7$, while the calculated value is lower for the thrust coefficient of aft propeller, which the average error is 8.227% and the maximum error reach 13.007% for $J=1.1$. The error of torque coefficient of forward propeller declines from 3.371% for $J=0.7$ to -5.756% for $J=1.1$ as the average error is -0.036%. The error of torque coefficient of the aft drops from 8.741% for $J=0.7$ to -1.601% for $J=1.1$. Thus the calculated error ranges from -1.285% for $J=0.9$ to -6.164% for total thrust coefficient and from 1.356% for $J=1.0$ to 6.129% for $J=0.7$ for total torque coefficient. In addition, the error of efficiency is gently under-predicted with up to -3.623% error and the average value is 2.661%.

Table 3. Comparison of the theoretical values at three mesh quantity

Mesh quantity(104)		Forward		Aft	
		K _{tf}	10K _{qf}	K _{ta}	10K _{qa}
246.8	Cal.	0.08223	0.08874	0.14612	0.16846
	Error(%)	-1.030%	-0.511%	-1.113%	-0.734%
300.0	Cal.	0.08138	0.08828	0.14449	0.16722
	Error(%)	-1.101%	-0.587%	-1.164%	-0.771%
518.0	Cal.	0.08133	0.08822	0.14442	0.16716
	Error(%)	-1.101%	-0.587%	-1.164%	-0.771%



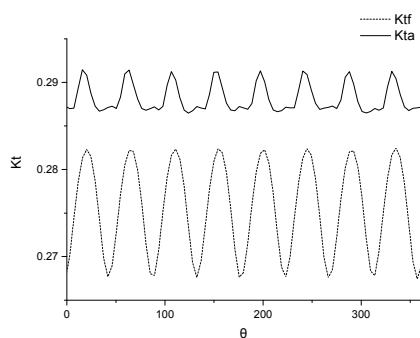
(a) forward propeller



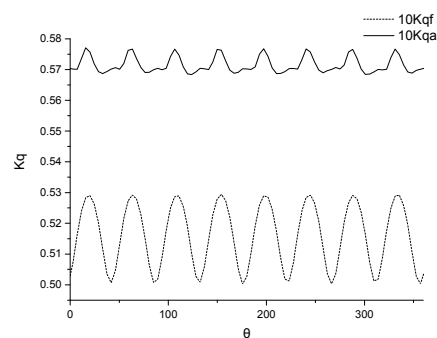
(b) aft propeller

Figure 3. Comparison of the numerical and experimental results

Figure shows the fluctuating thrust coefficient and torque coefficient of the forward and aft propellers when $J=0.7$. It can be clearly seen that both the thrust and torque coefficient fluctuate at a base frequency of 8 times the shaft frequency, which means the blades of each propeller meet once when they rotate by 45 degrees. et. The pulsation frequency of the thrust and torque coefficient can be expressed by $f = Z_F n_F + Z_A n_A$, where Z_F and Z_A are the blade number of the forward and aft propeller respectively; n_F and n_A are integers which satisfying $Z_F n_F = Z_A n$. Also, the coefficients of forward propeller expresses a stronger fluctuation than the aft in spite of lower values.



(a) thrust coefficient



(b) torque coefficient

Figure 4. Hydrodynamic performance in open water ($J=0.7$)

Fig.5 compares the computed pressure coefficient contours at different advance coefficient, i.e. $J=0.7, 0.9$ and 1.1 . Same legend and color levels are used in the sections of either fore propeller or aft propeller for comparison though the actual peak may exceed the range of legend in some plots. It can be seen that for the suction surfaces (a) and (c), the area where the pressure is low declines as J increases, while for the pressure surface (b) and (d), there is no significant change in the three cases. The minimum and the maximum appear at the leading edge on the suction surface and pressure surface respectively.

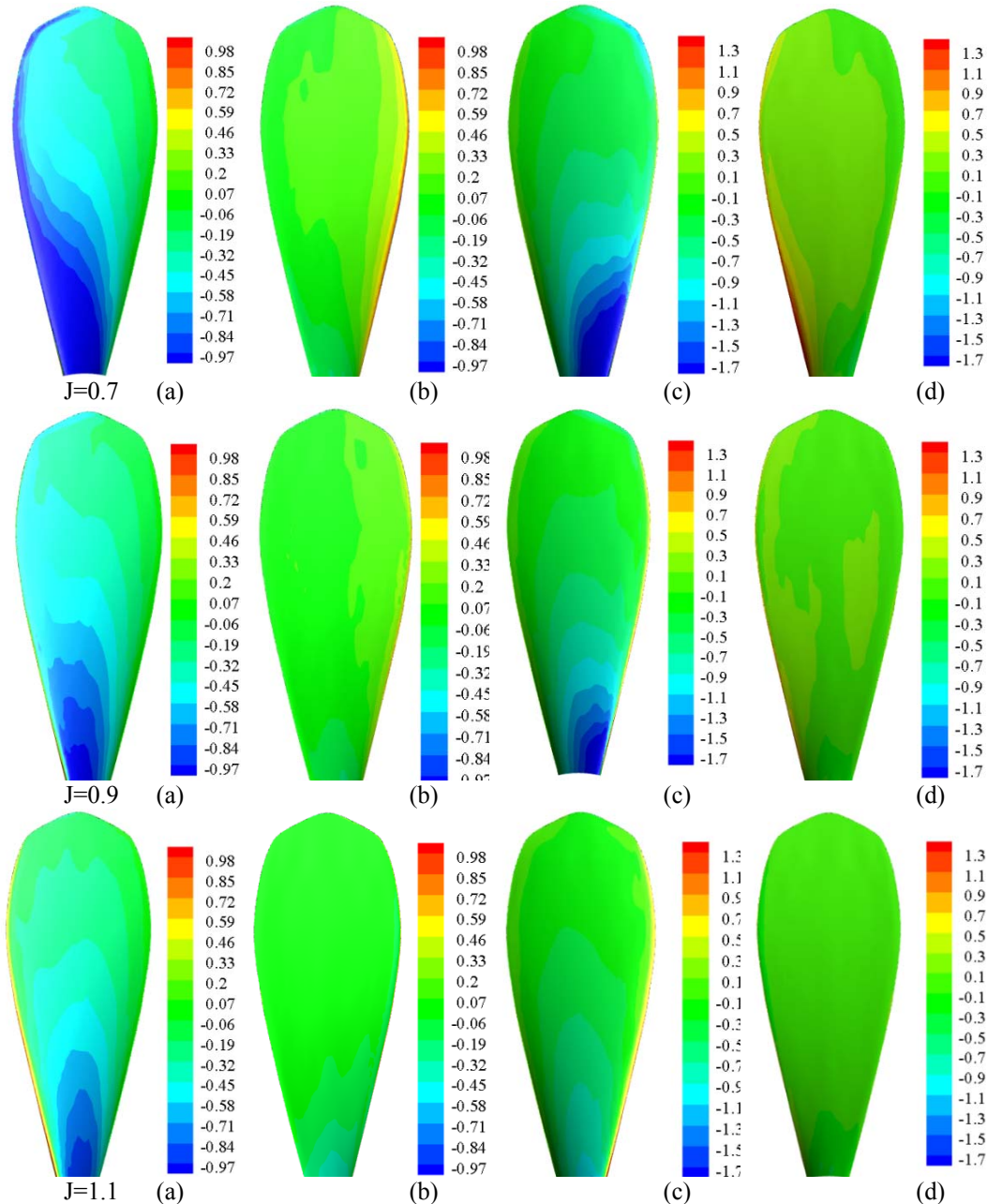


Figure 5. Comparison of C_p on both suction surface and pressure surface at different J values: $0.7, 0.9$ and 1.1 . (a) suction surface of fore propeller; (b) pressure surface of fore propeller; (c) suction surface of fore propeller and (d) pressure surface of fore propeller

Conclusions

In this paper, Star CCM+ is applied in the simulation of the hydrodynamic performance of contra rotating propellers. The numerical results is verified by the convergence study and the experimental data. Extensive simulation is performed to analyze the fluctuation of the propeller thrust and torque.

Acknowledgement

The authors are grateful for the support of the National Natural Science Foundation of China (Grant Nos. 51678045, 51579052).

References

- [1] C. J. Yang, M. Tamashima, G. Q. Wang, R. Yamazaki, Prediction of the Steady Performance of Contra-Rotating Propellers by Lifting Surface Theory, *The Japan Society of Naval Architects and Ocean Engineers*, 82(1991), 17-31
- [2] S. Tsakonas, W. R. Jacobs, P. Liao, Prediction of Steady and Unsteady Loads and Hydrodynamic Forces on Counterrotating Propellers, *J.S.R. Vol. 27, No. 3* (1983), 197–214
- [3] K. S. Min, B. J. Chang, H. W. Seo, Study on the Contra-Rotating Propeller system design and full-scale performance prediction method[J]. *International Journal of Naval Architecture and Ocean Engineering*, 2009, 1(1): 29-38.
- [4] A. Stuermer, Unsteady cfd simulations of contra-rotating propeller propulsion systems[J]. Paper No. AIAA-2008-5218, 2008.
- [5] C. Suryanarayana, M. N. Rao, P. N. Raju, Structural Analysis of a Contra Rotating Propeller by using Finite Element Method (FEM)[J]. *International Journal of Innovative Research and Development* | ISSN 2278–0211, 2015, 4(7), 80-92